GBF1, a cis-Golgi and VTCs-localized ARF-GEF, is implicated in ER-to-Golgi protein traffic

Xinhua Zhao[1], Alejandro Claude[1,*], Justin Chun[1], David J. Shields[1,‡], John F. Presley[2] and Paul Melançon[1,§]

[1]Department of Cell Biology, University of Alberta, Edmonton, Alberta, T6G 2H7, Canada
[2]Department of Anatomy and Cell Biology, McGill University, Montreal, Quebec, H3A 2B2, Canada
*Present address: Instituto de Bioquímica, Universidad Austral de Chile, Valdivia, Chile
‡Present address: Moores UCSD Cancer Center, La Jolla CA 92093-0803, USA
§Author for correspondence (e-mail: Paul.Melancon@ualberta.ca)

Accepted 18 July 2006
Journal of Cell Science 119, 3743-3753 Published by The Company of Biologists 2006
doi:10.1242/jcs.03173

Summary

The formation and maturation of membrane carriers that transport cargo from the ER to the Golgi complex involves the sequential action of the coat protein complexes COPII and COPI. Recruitment of COPI to nascent carriers requires activation of ADP-ribosylation factors by a BrefeldinA-sensitive guanine nucleotide exchange factor. Using new antisera and a GFP-tagged protein, we demonstrate that the exchange factor GBF1 localized to both Golgi membranes and peripheral puncta, near but separate from ER exit sites. Live cell imaging revealed that GFP-GBF1 associates dynamically with both membranes through rapid exchange with a large cytosolic pool. Treatment with BrefeldinA dramatically altered this rapid exchange, causing accumulation of GBF1 on both Golgi and peripheral puncta before eventual redistribution to the ER in a microtubule-dependent manner. Measurement of diffusion coefficients and subcellular fractionation confirmed this shift in GBF1 from cytosolic to membrane bound. BrefeldinA-induced accumulation of GBF1 coincided with loss of COPI from peripheral puncta. Furthermore, recruitment of GBF1 to cargo-containing peripheral puncta coincided with recruitment of COPI, but not COPII. Strikingly, microinjection of anti-GBF1 antibodies specifically caused dissociation of COPI from membranes. These observations strongly suggest that GBF1 regulates COPI membrane recruitment in the early secretory pathway.

Supplementary material available online at
http://jcs.biologists.org/cgi/content/full/119/18/3743/DC1

Key words: GBF1, ERGIC, VTCs, ARF-GEF, Brefeldin A, Protein traffic

Introduction

In mammalian cells, long-range transport of cargo proteins from peripheral ER exit sites (ERES) to the juxta-nuclear Golgi complex is mediated by pleiomorphic transport carriers called vesicular tubular clusters (VTCs) (Bannykh and Balch, 1997; Lee et al., 2004; Tang et al., 2005). In agreement with their function, VTCs localize both at the cell periphery (Hauri et al., 2000; Klumperman et al., 1998) and in the juxtanuclear region at the cis-face of the Golgi complex. The formation and maturation of VTCs requires the sequential action of two cytosolic coat protein complexes called COPII and COPI (Aridor and Balch, 1995). Current evidence suggests that ER cargo is selected at ERES into COPII-coated structures that subsequently bud and fuse to generate VTCs (Lee et al., 2004; Tang et al., 2005; Xu and Hay, 2004; Zeuschner et al., 2006). COPI complexes are then recruited 'en bloc' from the cytosol to nascent VTCs and remain associated with these pleiomorphic structures as they undergo their microtubule dependent movement toward the Golgi complex (Presley et al., 1997; Scales et al., 1997; Shima et al., 1999; Stephens et al., 2000). This model, however, does not explain the observation that treatment with the drug Brefeldin A (BFA), a fungal metabolite that blocks COPI but not COPII function (Bednarek et al., 1995; Donaldson et al., 1990; Klausner et al., 1992; Lippincott-Schwartz et al., 1989) prevents the COPII-driven accumulation of anterograde cargo at ERES structures (Altan-Bonnet et al., 2004; Ward et al., 2001). Current evidence therefore suggests that COPII function is tightly linked to, and dependent on, COPI recruitment on ERES structures (Altan-Bonnet et al., 2004; Ward et al., 2001).

COPI-coated transport carriers appear to be involved at several stages of the early secretory pathway (Rabouille and Klumperman, 2005). COPI was first identified on Golgi-derived coated vesicles (Orci et al., 1986; Waters et al., 1991) and subsequently localized to several compartments of the secretory pathway, with greatest abundance in VTCs and cis-elements of the Golgi stack (Griffiths et al., 1995; Oprins et al., 1993). Biochemical and morphological studies first documented its role in the formation of vesicular carriers from the Golgi complex (Orci et al., 1998; Orci et al., 1997; Ostermann et al., 1993), and subsequent experiments established that COPI plays an essential role in retrograde Golgi-to-ER transport (Letourneur et al., 1994; Majoul et al., 1998; Orci et al., 1997). Nevertheless, several lines of evidence support a role for COPI in anterograde transport from the ER to the Golgi complex. For example, antibodies against β-COP inhibited the transport of a temperature-restricted mutant form of the vesicular stomatitis virus (VSV) G protein (VSVG) from the ER to the Golgi complex both in vivo (Pepperkok et al., 1993) and in vitro (Peter et al., 1993). Furthermore, a CHO

(Chinese hamster ovary) cell line expressing a mutant form of ε-COP is defective in ER-Golgi transport at the non-permissive temperature (Guo et al., 1994). Proposed mechanisms include concentration of anterograde-moving cargo by exclusion from COPI-coated domains at VTCs (Martinez-Menarguez et al., 1999; Shima et al., 1999), or more direct involvement in sorting at VTCs in mammalian cells (Altan-Bonnet et al., 2004; Stephens and Pepperkok, 2002; Ward et al., 2001).

The recruitment of COPI to membranes depends on activation of small GTPases of the ADP-ribosylation factor (ARF: ADP-ribosylation factor) family. ARFs are found in the cytosol in the inactive GDP-bound form, and their activation by exchange of GDP for GTP is linked to a conformational change that dramatically increases their affinity for membranes (Goldberg, 1998). All ARF-specific guanine nucleotide exchange factors (GEFs) identified to date (Cox et al., 2004) possess a central Sec7 domain (Sec7d), a module of approximately 200 amino acids sufficient for GEF activity (Chardin et al., 1996; Mansour et al., 1999). A subset of these ARF-GEFs has been identified as the main cellular target of the inhibitor of COP1 function BFA (Melancon et al., 2004). BFA blocks the GEF activity of the Sec7d itself through an uncompetitive mechanism in which BFA traps the ARF substrate in a complex with the Sec7d (Mansour et al., 1999; Peyroche et al., 1999). Crystal structures subsequently revealed that BFA binds at the interface between the Sec7d and ARF•GDP, thus interfering with movement of the ARF core towards the Sec7d and freezing the Sec7d•Arf•GDP complex (Mossessova et al., 2003; Renault et al., 2003).

Outside of the Sec7d, ARF-GEFs display highly divergent peptide sequences that may play some role in targeting individual GEFs to specific membrane sites (Mouratou et al., 2005). Two subfamilies of large ARF-GEFs operate at the Golgi complex where they appear to perform distinct functions (Melancon et al., 2004). BIGs (BFA-inhibited GEFs) and their yeast ortholog Sec7p localize to trans-elements of the Golgi complex (Mogelsvang et al., 2004; Shinotsuka et al., 2002; Zhao et al., 2002). By contrast, GBF1 (Golgi-specific BFA resistance factor 1) and its yeast orthologs Gea1/2p associate with cis-Golgi elements (Garcia-Mata et al., 2003; Spang et al., 2001; Zhao et al., 2002). The domains responsible for targeting these large ARF-GEFs to specific compartments of the Golgi complex remain unknown.

Several lines of evidence support the possibility that GBF1 regulates COPI recruitment in early compartments of the secretory pathway. First, detailed localization studies revealed that GBF1 redistributes to peripheral VTCs at 15°C, as expected of an ARF-GEF that must be recruited de novo from a cytoplasmic pool to initiate COPI recruitment onto ER-derived VTCs (Kawamoto et al., 2002; Zhao et al., 2002). Second, overexpression of GBF1 antagonized the BFA-induced membrane dissociation of COPI (Claude et al., 1999; Kawamoto et al., 2002). Lastly, overexpression of the inactive GBF1 E794K mutant led to COPI dissociation from membranes (Garcia-Mata et al., 2003). However, direct evidence for the involvement of GBF1 in COPI membrane association has remained elusive. Furthermore, contrary to this predicted function in the membrane recruitment of COPI that is clearly BFA sensitive (Donaldson et al., 1991; Torii et al., 1995; Yan et al., 1994), GBF1 appeared resistant to BFA in biochemical assays of its GEF activity with purified components (Claude et al., 1999; Kawamoto et al., 2002).

In this study, we report that GBF1 exists in a large cytosolic pool that dynamically associates not only with membranes of the Golgi complex, but also with those of peripheral VTCs. GBF1 appears sensitive to BFA in vivo since BFA traps GBF1 on membranes and causes its accumulation at the Golgi complex, and on VTCs that appear close to, but physically separate from ERES. Microinjection of anti-GBF1 antibodies caused dissociation of COPI from membranes in vivo. These observations demonstrate that GBF1 is the BFA-sensitive ARF-GEF that regulates the dynamic association of COPI with VTCs for cargo transport between the ER and the Golgi complex.

Results

Endogenous GBF1 localizes to β-COP positive peripheral VTCs at steady state

To examine GBF1 function further, we raised several

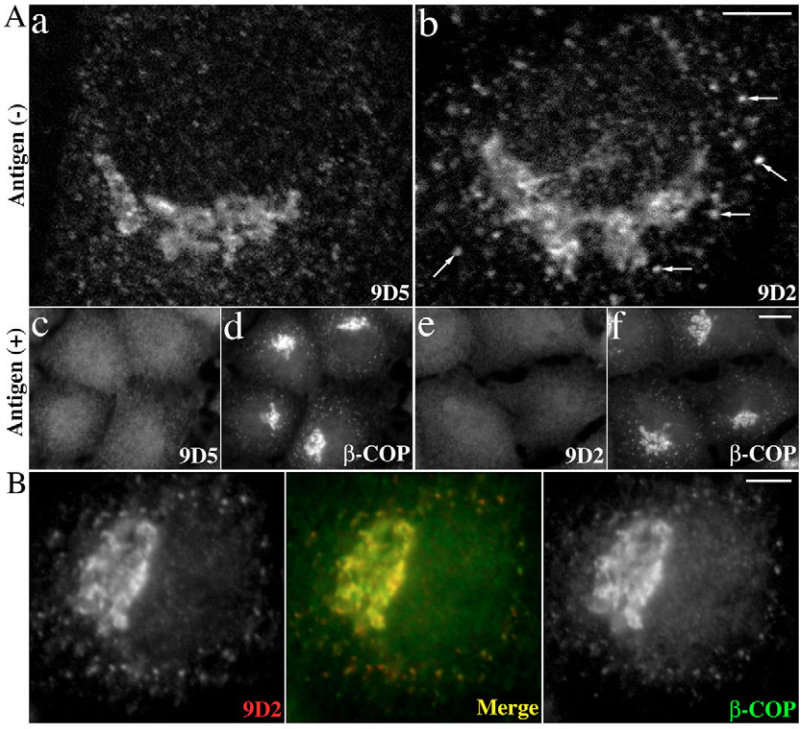

Fig. 1. Endogenous GBF1 localizes to β-COP positive peripheral VTCs at steady state. (A) Images a and b. NRK cells were fixed and processed for confocal IF using affinity-purified antibodies against GBF1 [9D5 (a) or 9D2 (b)]. Arrows mark peripheral 9D2-positive puncta. Bar, 5 μm. Images c-e. NRK cells were fixed and processed for standard IF in the presence of 1 μg GBF1 antigen using monoclonal anti-β-COP antibody and either 9D5 (c,d) or 9D2 (e,f). Bar, 10 μm. (B) NRK cells were fixed and processed for standard IF using affinity purified 9D2 and β-COP antibody. Bar, 5 μm.

additional polyclonal sera against recombinant fragments of hGBF1 (see Materials and Methods). One of these sera, 9D5, yielded primarily juxtanuclear signal (Fig. 1A, panel a), as previously reported with antiserum H-154 raised against a C-terminal peptide (Claude et al., 1999; Zhao et al., 2002). Although produced with the same immunogen, antiserum 9D2 reproducibly stained peripheral structures in addition to the juxta-nuclear region (arrows, Fig. 1A, panel b). To confirm the specificity of the peripheral staining we examined the impact of excess immunizing protein on 9D2 and 9D5 staining. As shown in Fig. 1A (panels c-f), antigen completely eliminated GBF1 signal to both the juxtanuclear region and peripheral puncta, but had no impact on co-staining with monoclonal antibodies against β-COP. To determine if GBF1-positive puncta correspond to peripheral VTCs, we examined if they also contained the VTC marker β-COP (Griffiths et al., 1995; Oprins et al., 1993). GBF1 co-localized significantly with β-COP in peripheral puncta (Fig. 1B), confirming that GBF1 localizes to VTCs where it may regulate COPI recruitment.

GBF1 exchanges rapidly between free cytosolic and membrane-bound pools in live cells

To study GBF1 dynamics in vivo, we generated normal rat kidney (NRK) cell lines stably expressing chimeras containing the enhanced variant of GFP (EFGP) fused to the N-terminus of full length CHO-derived GBF1 (GFP-GBF1, Fig. 2A; see Materials and Methods). Like endogenous GBF1, GFP-GBF1 localized primarily to a juxta-nuclear structure, but also to small peripheral puncta (arrowheads; Fig. 2B panels a,d,g). As previously established for GBF1 (Zhao et al., 2002), GFP-GBF1 co-localized with the cis-Golgi localized protein, p115, but remained separate from the TGN localized protein, BIG1 (Fig. 2B). Similarly, as observed for the endogenous protein (Fig. 1B), GFP-GBF1-positive peripheral puncta also contained COP1 (Fig. 2B panels g-i). Expression levels varied widely in the population and proper localization was observed even within cells that significantly overexpressed GFP-GBF1 above endogenous levels (our unpublished data). GFP-GBF1 also appeared functional since as observed with full-length GBF1 (Claude et al., 1999), overexpression permitted growth in the presence of BFA (our unpublished data). These observations established that GFP-GBF1 could be used to examine the localization and behavior of GBF1 in living cells, and further confirmed that a significant amount of GBF1 localizes to VTCs.

Endogenous and GFP-tagged GBF1 both displayed diffuse staining over the entire cytoplasm. To determine whether this staining corresponded to free cytosolic protein, or poorly resolved reticular membranes, we performed fluorescence recovery after photobleaching (FRAP) experiments. Signal recovery in photobleached areas distant from the juxtanuclear region occurred very rapidly, and appeared complete 10 seconds following bleach (Fig. 3A). Analysis of recovery kinetics from several experiments yielded a diffusion coefficient (D) of 0.95±0.13 $\mu m^2\ s^{-1}$ (n=8), a value consistent with that of a free protein and significantly greater than D values reported for Golgi associated proteins [0.3-0.5 $\mu m^2\ s^{-1}$ (Cole et al., 1996)] or the largest D known for a membrane protein, that of rhodopsin [0.5 $\mu m^2\ s^{-1}$ (Wey et al., 1981)]. This observation confirms our previous observations that a

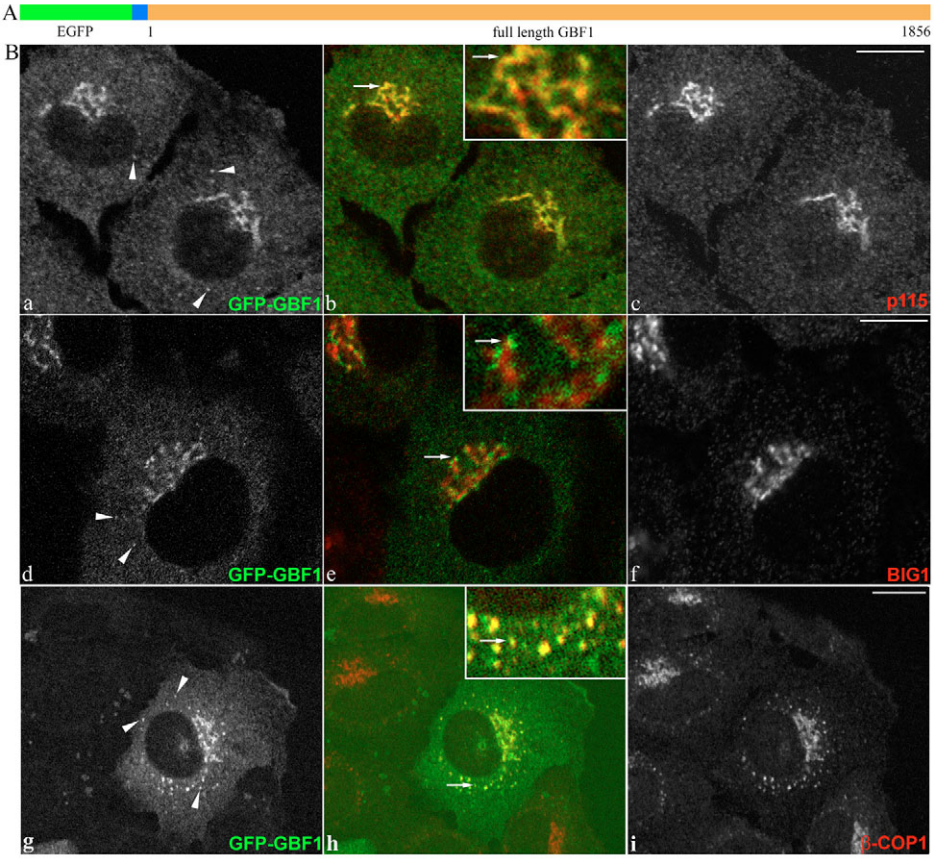

Fig. 2. GFP-GBF1, like endogenous GBF1, is recruited to cis-Golgi membranes and peripheral VTCs membranes. (A) Schematic representation of GFP-GBF1: EGFP (green) was fused in frame with full length CHO-derived GBF1 (orange) at its N terminus. Additional residues encoded by plasmid-derived and UTR sequences shown in blue. (B) NRK cells stably expressing GFP-GBF1 were fixed and processed for either double-label confocal IF by staining with affinity purified polyclonal antibody against GFP (a) and monoclonal antibody against p115 (3A10) (c) or single-label IF by staining with polyclonal antibody against BIG1 (9D3) (f) or monoclonal antibody against β-COP (M3A5) (i). Arrowheads mark puncta revealed by GFP fluorescence (d,g) or GFP antibodies (a). Middle panels (b,e,h) show merged left and right images. Insets show threefold magnification of the area indicated by arrow. Bars, 10 μm.

significant pool of GBF1 in homogenates is soluble (Claude et al., 1999) (see also Fig. 4C).

To determine whether the cytosolic and membrane pools are in dynamic equilibrium, we repeated FRAP experiments on membrane bound GFP-GBF1. Following photobleaching of juxtanuclear Golgi-associated signal, we observed rapid fluorescence recovery (Fig. 3B). Quantitative analysis of several independent FRAP experiments (see Materials and Methods) revealed that the fraction of fluorescence signal in the juxtanuclear region (termed Golgi-to-cell ratio) averaged about 15%. The majority (81±1.3% n=10) of Golgi-bound GBF1 appeared mobile and recovered exponentially to near pre-bleach levels with an average half time ($t_{½}$) of 16.0±1.9 seconds (n=10) (Fig. 3C). This rate is similar to that previously reported for ARF1-GFP and significantly faster than the $t_{½}$ of 35 seconds measured for COPI (Presley et al., 2002). FRAP kinetics of Golgi-associated GFP-GBF1 were not affected by disruption of microtubules with nocodazole (NOZ) (Fig. 3D), a treatment previously shown to block anterograde movement of peripheral VTCs (Presley et al., 1997). We concluded that

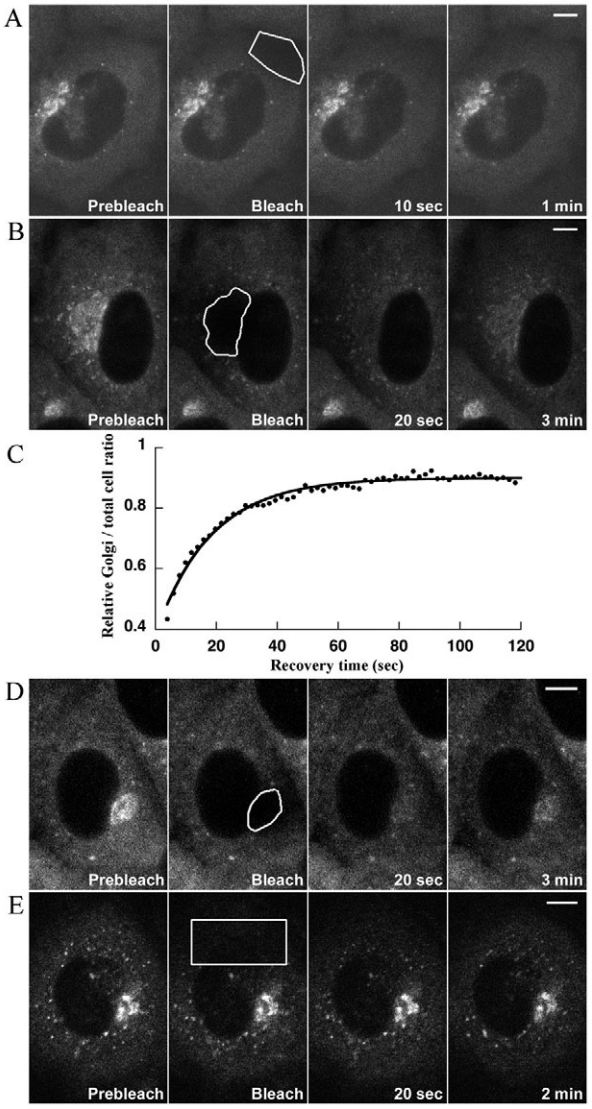

Fig. 3. Kinetics of GBF1 binding to and dissociation from Golgi and VTCs membranes in NRK cells stably expressing GFP-GBF1. Live NRK cells expressing GFP-GBF1 were examined by confocal microscopy at 37°C as described in Materials and Methods. (A) Cytosol FRAP was performed as described in Materials and Methods. Shown are still images at the indicated times. (B) Golgi FRAP. Experiment similar to that shown in 3A except that the ROI includes the Golgi complex. (C) Quantification of the Golgi FRAP experiment presented in 3B. The curve was obtained by fitting FRAP data to a single exponential corresponds to the equation: y=0.520 * (1-$e^{-0.055t}$) + 0.381 with an R value of 0.991. (D) Golgi FRAP in absence of microtubules. FRAP analysis was performed as in 3B, except that cells were chilled on ice for 15 minutes and warmed to 37°C in the presence of 1 μg ml^{-1} NOZ. (E) VTCs FRAP. Similar to experiment shown in 3B except that the ROI was located in the cell periphery and contained GBF1-positive VTCs. Bars, 5 μm.

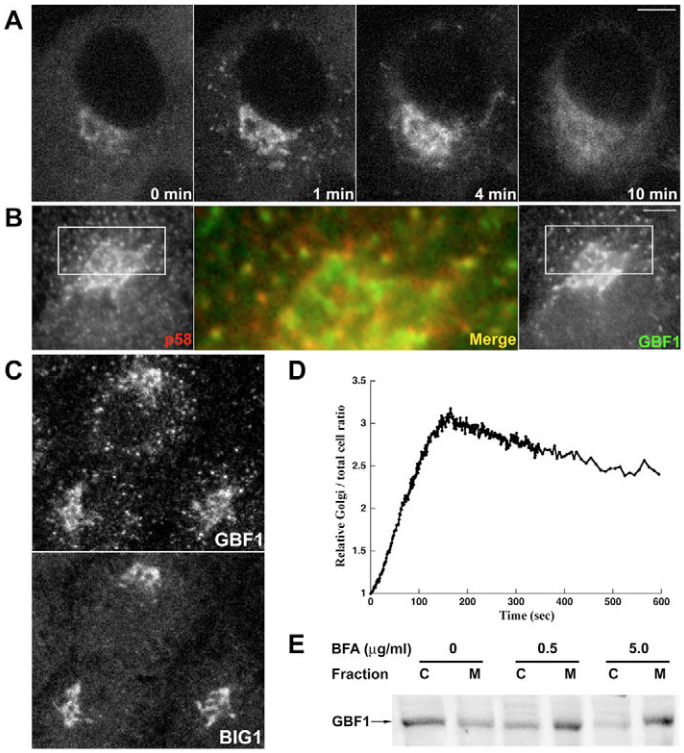

Fig. 4. GBF1 accumulates on membranes of the Golgi complex and peripheral VTCs upon treatment with BFA. (A) Images of NRK cells expressing GFP-GBF1 were captured every 2 seconds for 10 minutes immediately after BFA addition (1 μg ml^{-1}). Still images from indicated time points illustrate the transient accumulation of GBF1 onto peripheral VTCs and Golgi complex. (supplementary material Movie 1). Bar, 5 μm. (B) NRK cells treated with BFA (5 μg ml^{-1}) for 30 seconds were fixed and processed for standard IF using Alexa488-conjugated anti-GBF1 rabbit antibody (H-154) and rabbit anti-p58 antibodies. Merged image shows threefold magnification of boxed area in red and green channels. Bar, 5 μm. (C) NRK cells treated with 5 μg ml^{-1} BFA for 1 minute were fixed and processed for confocal IF using polyclonal antibodies against GBF1 (H154) and BIG1 (Alexa488-conjugated 9D3). Bar, 10 μm. (D) Quantification of experiment 4A showing Golgi/total ratio plotted against treatment length. (E) NRK cells were washed in ice-cold buffer containing either DMSO vehicle control (0), or 0.5 μg ml^{-1} (0.5) or 5 μg ml^{-1} (5.0) BFA. Cytosol (C) and microsomes (M) fractions were prepared and analyzed for GBF1 content by immunoblot (see Materials and Methods).

recovery was mediated not by delivery via cargo carriers but by exchange with free cytosolic GBF1. FRAP experiments on peripheral VTCs revealed that GFP-GBF1 also rapidly exchanged on and off these structures (Fig. 3E).

BFA causes accumulation of GBF1 on VTC and Golgi membranes

Previous work established that GBF1 redistributed from the Golgi complex to a diffuse pattern following prolonged treatment with BFA (Garcia-Mata et al., 2003; Kawamoto et al., 2002; Zhao et al., 2002). Time-lapse imaging revealed that GFP-GBF1 accumulated transiently on both peripheral puncta and the juxtanuclear Golgi area prior to its eventual redistribution (Fig. 4). Addition of BFA (1 μg ml^{-1}) caused accumulation of GBF1 in a large number of puncta as early as 10 seconds, reaching maximal signal after 1 minute. Signal 'blinked out' abruptly from various peripheral sites over the following 4 minutes (Fig. 4A and supplementary material Movie 1), apparently redistributing into a reticular network likely corresponding to the ER (see below).

Analysis of several time-lapse movies suggests that BFA-induced accumulation occurred on structures positive for GBF1 prior to drug addition. To confirm the identity of these structures, we compared GBF1 distribution to that of ERGIC53/p58, a well-characterized VTC marker (Saraste et al., 1987). BFA treatment of standard NRK cells caused accumulation of endogenous GBF1 onto puncta similar to that observed for GFP-GBF1 (Fig. 4B). Most GBF1 positive puncta also stained for p58, and the two proteins co-localized significantly in those structures. In sharp contrast, no BIG1 accumulated in peripheral structures (Fig. 4C). These results suggest that GBF1, but not BIG1, normally functions at VTCs.

GBF1 recruitment in the juxtanuclear region proceeded over a time period longer than observed at VTCs (Fig. 4A and supplementary material Movie 1). Quantification of Golgi-to-cell ratio as a function of time after BFA addition (1 μg ml^{-1}) revealed a gradual threefold increase of the Golgi signal within 3 minutes (Fig. 4D). Subsequent decrease in signal coincided with redistribution of GFP-GBF1 from the Golgi complex to a diffuse pattern (Fig. 4A,D). Raising BFA concentration from 0.3 to 1.0 μg ml^{-1} greatly increased the rate of accumulation and, as previously reported for Golgi resident enzymes (Lippincott-Schwartz et al., 1989), significantly shortened the lag before redistribution of GFP-GBF1 to a reticular ER pattern (our unpublished data).

To confirm the BFA-induced recruitment of GBF1 onto membranes, we performed subcellular fractionation on homogenates prepared from NRK cells treated with BFA prior to disruption. As previously observed (Claude et al., 1999), the cytosolic fraction of mock-treated cells contained most GBF1 (>80%) (Fig. 4E). Treatment with BFA for a few minutes on ice at a concentration as low as 0.5 μg ml^{-1} caused a dramatic change in distribution. As predicted from the FRAP data on live cells, treatment with a higher BFA concentration caused near complete association of GBF1 with the microsomal pellet.

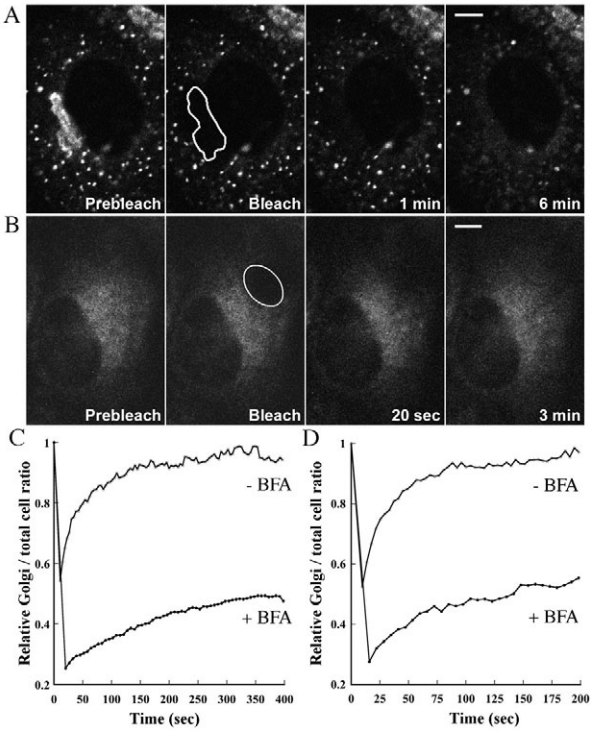

Fig. 5. BFA treatment traps GBF1 onto membranes. (A) NRK cells expressing GFP-GBF1 were incubated on ice for 15 minutes with 5 μg ml^{-1} NOZ prior to transfer onto microscope stage (37°C). Following equilibration, BFA (5 μg ml^{-1}) was added and FRAP performed as for 3B. Bar, 5 μm. (B) FRAP was performed as for 3A except that cells were treated with 5 μg ml^{-1} BFA for 10 minutes prior to bleach. ROI size was similar to that used for untreated cells in Fig. 3A. Bar, 5 μm. (C) Quantification of panels 5A (+BFA) and 3D (–BFA) showing relative Golgi/total ratio plotted against treatment length. (D) Quantification of panels 5B (+BFA) and 3A (–BFA) showing relative Golgi/total ratio plotted against treatment length.

BFA prevents dynamic exchange between membrane-bound and cytosolic GBF1 pools

To determine whether the effect of BFA on GBF1 distribution resulted from faster association or slower dissociation, we examined the recovery rate after Golgi photobleaching in the presence of BFA. Cells were pre-treated with NOZ for 15 minutes on ice to disrupt microtubules before BFA addition; NOZ had no impact on recovery kinetics (Fig. 3D), but delayed the microtubule dependent BFA-induced redistribution of GBF1 to the ER long enough to allow measurement of recovery kinetics (Sciaky et al., 1997). A series of images from representative time points is shown in Fig. 5A. While the majority of GFP-GBF1 signal returned to the bleached Golgi area within a minute in control cells (Fig. 3D), very little recovery occurred even after 6 minutes in the presence of BFA (Fig. 5A). Quantitative analysis of the FRAP data presented in Fig. 3D, Fig. 5A confirmed the much slower exchange rate upon BFA treatment (Fig. 5C).

After prolonged BFA treatment, GBF1 redistributed to a diffuse pattern that could represent either free or ER membrane bound GBF1. To distinguish between these possibilities we performed FRAP experiments on cells treated BFA (5 μg ml^{-1}) for 30 minutes. Whereas we had observed almost immediate recovery for untreated cells (Fig. 3A, Fig. 5D), it took as long as 3 minutes for less than 50% recovery in BFA treated cells (Fig. 5B,D). Whereas GBF1 diffused with a rate of 0.95±0.13 (n=8) consistent with that of a soluble protein in untreated cells

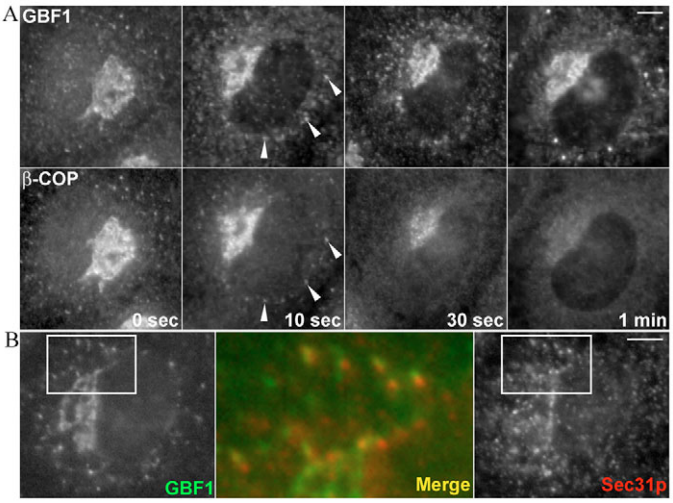

Fig. 6. BFA-induced accumulation of GBF1 coincides with loss of COPI from peripheral VTCs that lie in close proximity to Sec31p-positive structures. (A) NRK cells treated with BFA (5 μg ml^{-1}) for various times (0; 10 seconds; 30 seconds and 1 minute) were fixed and processed for standard IF using anti-GBF1 rabbit antibody (9D2) and anti-β-COP mouse antibodies (M3A5). White arrowheads mark puncta containing both GBF1 and β-COP. (B) NRK cells treated with BFA (5 μg ml^{-1}) for 30 seconds were fixed and processed for standard IF using Alexa488-conjugated anti-GBF1 rabbit antibody (H-154) and rabbit anti-sec31p antibodies. Merged image shows a threefold magnification of boxed area in red and green channels. Bars, 5 μm.

(see above), analysis of several FRAP experiments as Fig. 5B yielded a rate of 0.21±0.03 (n=8). Such a dramatic decrease in mobility is consistent with GBF1 remaining membrane-associated after prolonged BFA treatment (Cole et al., 1996; Presley et al., 2002).

GBF1- positive peripheral structures lie close to but appear physically separate from ERES

To probe the proposed function of GBF1 on peripheral structures, we examined in more detail its distribution relative to that of the COPI subunit β-COP and the COPII subunit Sec31p. Whereas COPII functions at ERES and appears stationary (Stephens et al., 2000), COPI decorates VTCs that can be motile but are often juxtaposed to COPII-positive structures (Presley et al., 1997; Scales et al., 1997). As shown in Fig. 6A, at early time points (10 seconds) following BFA addition when β-COP largely remains membrane-associated, some GBF1 already accumulated on β-COP-positive peripheral puncta (Fig. 6A). Consistent with previous observations (Donaldson et al., 1990; Scheel et al., 1997; Presley et al., 2002), most COPI dissociated from membranes within 1 minute. Interestingly, GBF1-positive puncta appeared not to overlap with, but instead lie in close proximity to Sec31p-positive structures (Fig. 6B).

The BFA-induced accumulation of GBF1 onto nascent VTCs allowed us to address the model in which GBF1 initiates recruitment on membranes directly connected to ERES, prior to release of VTCs (Altan-Bonnet et al., 2004; Ward et al., 2001). We reasoned that disruption of the microtubule network by brief treatment with NOZ would prevent separation of VTCs from ERES and accelerate the collapse of transient GBF1-positive puncta. To our surprise, microtubule disruption had the opposite effect. In NOZ-treated cells, endogenous GBF1 accumulated as before, but rather than dispersing into the ER within 3 minutes of BFA addition, it remained associated with most peripheral structures for more than 10 minutes (Fig. 7 and supplementary material Movie 2). NOZ caused similar stabilization of endogenous GBF1-positive puncta in HeLa and COS cells (unpublished data). These observations demonstrate that most peripheral VTC structures onto which GBF1 accumulates are physically separate from ERES.

GBF1 participates in ER-Golgi traffic by regulating COPI recruitment

To investigate in more detail when GBF1 is recruited for anterograde cargo transport, we next examined the appearance of GBF1 on transport carriers containing tsO45-G, a temperature-sensitive mutant viral glycoprotein produced by

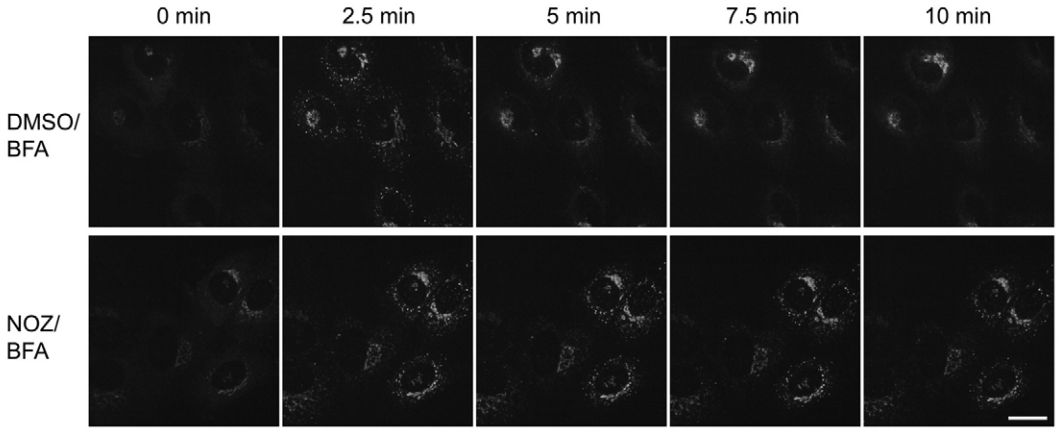

Fig. 7. Nocodazole (NOZ) treatment stabilizes GBF1-positive peripheral VTCs. NRK cells expressing GFP-GBF1 were treated on ice for 15 minutes with either 20 μg ml^{-1} NOZ or 0.5% DMSO. Following a 2 minute warm-up at 37°C, live cells were examined at 37°C on a Zeiss Axiovert 200M spinning disk microscope. Z-stacks of 6 slices each 1 μm thick were acquired continuously after addition of BFA (5 μg ml^{-1}). See supplementary material Movie 2. Still images from projected stacks at indicated times are shown. Bar, 20 μm.

vesicular stomatitis virus (VSV). tsO45-G accumulates in the ER at the restrictive temperature, can be synchronously released for export by temperature shift, and has been used extensively to dissect the molecular machinery of ER-to-Golgi transport (Bergmann, 1989; Kreis and Lodish, 1986). tsO45-G, like other cargo molecules, is initially sorted into COPII-coated ER export carriers and then transported from the ER to the Golgi in mobile VTCs that contain COPI (Presley et al., 1997; Scales et al., 1997). Quantitative analysis (Scales et al., 1997) revealed that the peak of co-localization between tsO45-G and COPII occurred earlier (~1 minute after temperature shift) than that with COPI (>6 minutes).

To compare the localization of GBF1 with tsO45-G during its export from the ER, COS-1 cells infected with tsO45-VSV were kept at the restrictive temperature (40°C) for 3 hours, and then shifted to the permissive temperature (32°C) for either 1 minute or 6 minutes to allow synchronized ER export. As shown in Fig. 8, GBF1, like COPI, co-localized with VSVG in peripheral structures at later time points (6 minutes, image k) after temperature shift, but not at earlier time points (1 minute, image h), when COPII-dependent events lead to VTC formation. These observations suggest that GBF1 is recruited to the cargo-containing VTCs rather than to the earlier ER-associated cargo exit sites.

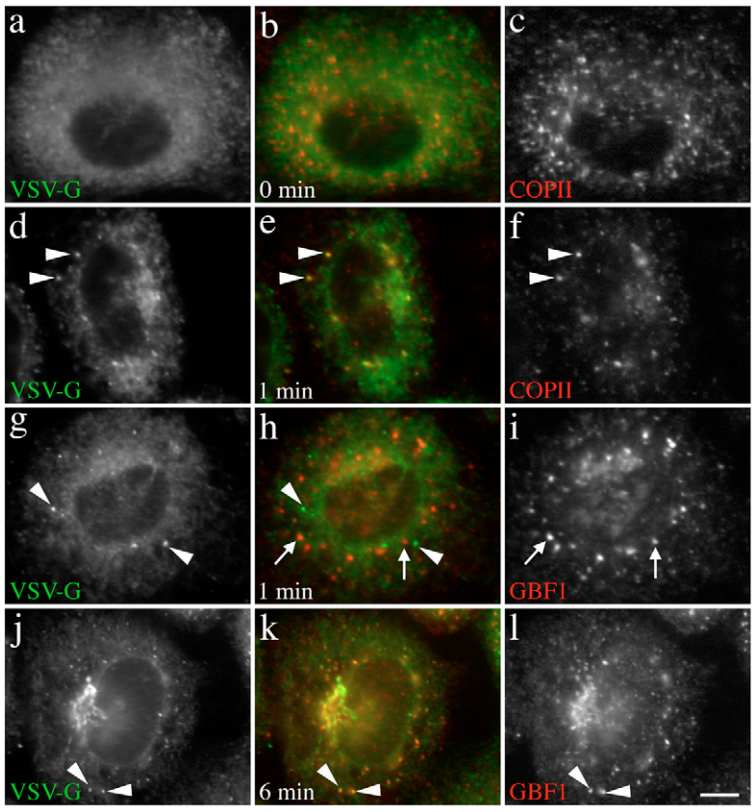

Fig. 8. GBF1 decorates matured VTCs labeled by VSVGtsO45. COS-1 cells infected with VSV tsO45 were incubated at 40.5°C for 3 hours (0 min) (a-c) and then shifted to permissive temperature 32°C for either 1 min (d-i) or 6 minutes (j-l). Cells were fixed and then processed for standard IF using monoclonal antibodies against VSVG (a,d,g,j) and polyclonal antibodies against either COPII (c,f) or GBF1 (i,l). Middle panels (b,e,h,k) show merged left and right images. Bar, 5 μm.

To investigate further the functional link between GBF1 and COPI, we targeted GBF1 function by microinjection of affinity-purified antibodies and analyzed the effect on COPI recruitment. Several anti-GBF1 antibodies were affinity-purified and microinjected into the cytoplasm of HeLa cells. Microinjected cells were identified by staining with a conjugated anti-rabbit antibody and the potential effects on COPI recruitment were assayed by staining for β-COP 2 hours post-microinjection. Only two out of four concentrated antibody preparations, 9D2 and 9D7, caused dissociation of COPI. As shown in Fig. 9, 9D2 was particularly effective, causing complete dissociation of COPI even at low level of microinjected antibodies. By contrast, 9D7 caused COPI dissociation only in cells that received high levels (our unpublished data). This effect was COPI-specific because anti-GBF1 antibodies microinjection did not disrupt the distribution of clathrin coats (Fig. 9, bottom panels). These results argue strongly that GBF1 is the ARF-GEF responsible for activating ARFs to initiate COPI membrane recruitment at peripheral VTCs.

Discussion

The ability of GBF1 to redistribute from the cis-Golgi to peripheral structures at 15°C led us to further explore a potential role for GBF1 in protein transport between the ER and Golgi complex. New antisera localized endogenous GBF1 not only to juxta-nuclear cis-Golgi membranes, but also to peripheral VTCs. FRAP studies established that GFP-GBF1 associated dynamically with both membranes with rapid exchange between a large cytosolic pool and a membrane-bound fraction. Treatment with BFA dramatically altered this rapid exchange, resulting in transient accumulation of GBF1 on both Golgi and VTC membranes. Subcellular fractionation and measurement of diffusion coefficients confirmed this shift from soluble to membrane-bound, and suggested that BFA traps GBF1 on an integral membrane protein that may act as compartment specific receptor. GBF1-positive VTCs appeared close to, but physically separate from Sec31p-decorated ERES. Recruitment of GBF1 to cargo-containing VTC structures coincided with recruitment of COPI, but not COPII. More importantly, microinjection of anti-GBF1 antibodies specifically caused dissociation of COPI from the membrane. These observations strongly suggest that GBF1 is the BFA-sensitive ARF-GEF that regulates membrane recruitment of COPI in the early secretory pathway.

GBF1, a largely cytosolic protein in dynamic equilibrium with a membrane-bound pool

Subcellular fractionation studies established that the vast majority of GBF1 appears in the cytosolic fraction of cellular homogenates (see Fig. 4E) (Claude et al., 1999). Imaging of GFP-GBF1 in live cells revealed approximately 85% of GBF1 in a diffuse pattern over the entire cytoplasm. FRAP analysis of this diffuse fraction yielded values of diffusion coefficient for GBF1 consistent with those expected of a free protein, confirming that indeed a significant

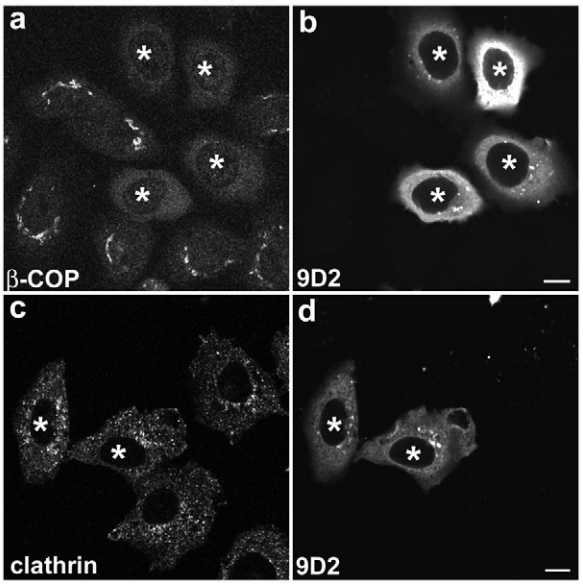

Fig. 9. Microinjection of anti-GBF1 antibodies specifically causes membrane dissociation of the COPI but not the clathrin coat. HeLa cells were microinjected with affinity-purified polyclonal anti-GBF1 antibodies (9D2), and fixed 2 hours post-injection. Microinjected cells, identified using goat anti-rabbit antibody, are indicated by white stars. COPI or clathrin coats were revealed using anti-β-COP (M3A5) or anti-clathrin (X22) monoclonal antibodies. Bars, 10 μm.

pool of GBF1 is soluble. Recently published studies revealed similar cytosolic pools of GFP-tagged forms of GBF1 (Niu et al., 2005; Szul et al., 2005), but those authors did not provide quantitative estimates of either its abundance or mobility.

FRAP experiments examining GFP-GBF1 dynamics in the juxta-nuclear Golgi region established that GFP-GBF1 rapidly exchanges on and off the membranes of the Golgi complex. While this manuscript was in preparation, similar results showing GBF1 membrane dynamics were reported (Niu et al., 2005; Szul et al., 2005). The $t_{1/2}$ of 16 seconds for GBF1 recovery determined by our FRAP analysis is similar to the $t_{1/2}$ (17 seconds) reported by one group (Szul et al., 2005), and both are significantly faster than the $t_{1/2}$ (30 seconds) reported by another (Niu et al., 2005). This variance could result from differences in experimental systems, especially different cell lines, type of GFP chimera and/or expression levels. We carried our FRAP analysis using a cell line stably expressing low to moderate amounts of GFP tagged GBF1 that is closer to physiological conditions, while the other two groups used transiently transfected cells with a wide range of expression level. High overexpression level of GBF1, sufficient to cause resistance to BFA-induced Golgi disassembly (Niu et al., 2005), might have altered GBF1 membrane dynamics and caused a slower $t_{1/2}$.

GBF1 is a BFA sensitive ARF-GEF in vivo

GBF1 was originally identified as BFA-resistant based on its BFA-resistant GEF activity toward ARF5 in an in vitro GEF assay (Claude et al., 1999). In addition, overexpression of GBF1 allowed cell growth in the presence of BFA at concentrations toxic to wild type cells. However, the demonstration in this paper and in two other recent reports (Niu et al., 2005; Szul et al., 2005) that BFA promotes recruitment of GBF1 onto Golgi membranes clearly establishes that GBF1 is a BFA target in the early secretory pathway. Membrane accumulation resulted from slower dissociation rather than increased association since all three groups report much longer residence time for GBF1 on Golgi membranes in the presence of BFA (see Fig. 5). Jackson and colleagues observed that BFA no longer altered the dynamics of a GFP-GBF1 mutant lacking potential BFA contact sites, and therefore confirmed that GBF1 was a direct target of the drug (Niu et al., 2005).

We suggest that the uncompetitive nature of BFA inhibition and the low concentrations of GBF1 and ARF substrate used in our original in vitro GEF assays (Claude et al., 1999) may be responsible the apparent BFA-resistance observed in vitro. Indeed, we subsequently discovered that reducing ARF levels in in vitro GEF assays causes a significant increase in the amount of BFA needed to observe inhibition (Mansour et al., 1999). The BFA resistance conferred by GBF1 overexpression likely results from compensation by increased total enzyme level for drug-reduced enzyme activity.

GBF1 regulates COPI membrane recruitment at VTCs

EM studies that localized a small but significant fraction of GBF1 on vesicular and tubular structures near the cis-face of Golgi stacks first suggested that this ARF-GEF could function on ER-Golgi carriers (Claude et al., 1999; Kawamoto et al., 2002). The observation that GBF1 partially redistributed to peripheral VTCs after incubation at 15°C provided additional support for this possibility (Kawamoto et al., 2002; Zhao et al., 2002). We have now confirmed using a GFP-tagged form and the new anti-GBF1 9D2 serum that GBF1 localizes to peripheral structures at steady state under normal physiological conditions.

The GBF1-positive peripheral structures are near to but appear physically separate from ERES. IF analysis established that GBF1 overlaps with the ERGIC marker p58 but appears largely separate from the ERES marker Sec31p. This result appears inconsistent with the observation that a myc-tagged form of GBF1 localizes to COPI-coated structures, the majority of which (66%) contained the COPII subunit Sec31p (Garcia-Mata et al., 2003). The apparent physical separation between COPII-positive ERES and the GBF1-positive peripheral VTCs we observe is further supported by the observation that NOZ treatment did not accelerate but rather blocked the fusion of the GBF1-positive VTCs with the ER following BFA treatment. This observation not only provides evidence for the lack of VTC-ERES continuity proposed by Lippincott-Schwartz and colleagues (Altan-Bonnet et al., 2004; Ward et al., 2001), but also uncovered the existence of a potential microtubule-dependent mechanism for retrograde movement of material from peripheral VTCs back to the ER.

The presence of GBF1 at peripheral VTCs in close proximity to ERES strongly suggests that it is the ARF-GEF responsible for initiation of ARF activation and recruitment of the COPI coat onto nascent cargo carriers. Our observation that membrane recruitment of GBF1 to cargo-containing VTC structures coincided with the recruitment of COPI, but not COPII (see Fig. 8), further supports this notion. However, our microinjection experiments with anti-GBF1 neutralizing antibodies provides the most convincing evidence: affinity-

purified 9D2 specifically caused dissociation of COPI from VTCs and Golgi membranes, while leaving clathrin intact in the juxtanuclear region (see Fig. 9) within 2 hours of microinjection. By contrast, previous experiments with the E794K mutant involved 12-14 h incubation to allow accumulation of sufficient levels of mutant proteins in cells transiently transfected with E794K constructs (Garcia-Mata et al., 2003). The phenotype observed under these conditions could have resulted from indirect effects. Clear loss of COP1 staining within 2 hours of microinjection greatly enhances the likelihood that the specific dissociation of COPI from membranes resulted directly from blocking GBF1 function.

BFA traps drug-sensitive ARF-GEFs on organelle-specific receptors

Our previous demonstration that the largely soluble GBF1 and BIGs are recruited to distinct Golgi sub-compartment first suggested the presence of 'receptors' whose localization and/or activity had to be tightly regulated. Following treatment with BFA, GBF1, but not BIG1, accumulated on peripheral VTCs (Fig. 4C). Furthermore, while GBF1 eventually redistributed to ER membranes (Fig. 5B,D), the membrane-bound BIG1 appeared in a hybrid organelle that clustered near the microtubule-organizing center in the presence of BFA (Zhao et al., 2002). This distinct behavior of GBF1 and BIG1 in response to BFA treatment, not only extends our original observation but may also provide important insights into the mechanism regulating their membrane recruitment.

Previous structural and biochemical analysis of the Sec7d•BFA•Arf•GDP complex demonstrates that BFA binding prevents GDP release but should not significantly alter association of the complex with membranes (reviewed in Cherfils and Melancon, 2005): the ARF•GDP-bound Sec7d should simply display the same cytosol to membrane distribution as ARF•GDP (Beraud-Dufour et al., 1999). Since BFA causes rapid release of the majority of ARF1 from Golgi membranes (Presley et al., 2002), the abortive Sec7d•BFA•Arf•GDP complexes were predicted to be largely soluble (Cherfils and Melancon, 2005). The clear BFA-induced recruitment of the GBF1 and BIGs to distinct compartments must therefore involve some other, compartment-specific membrane-associated component. The relatively small diffusion coefficient (0.21 ± 0.03 μm^2 s^{-1}) we measured for GBF1 following prolonged BFA treatment is significantly smaller than that of several integral membrane proteins in the Golgi complex (0.3-0.5 μm^2 s^{-1}) (Cole et al., 1996) and strongly supports this possibility.

Although the mechanisms regulating the association of GBF1 and BIG1 with their specific membrane receptors remain unknown, it is tempting to speculate that dissociation of the ARF-GEF complex from their receptor could be coupled to GDP release and/or subsequent GTP-binding (Cherfils and Melancon, 2005). Being unable to release GDP, the abortive Sec7d•BFA•Arf•GDP complex would remain bound to their membrane receptors. As predicted by this model, GBF1 (E794K) and ARF (T31N) mutants, known to stabilize the GBF1•Arf complex, promoted membrane association (Szul et al., 2005). Identification of the putative membrane receptors for GBF1 and BIGs will be required to ultimately test this model.

Materials and Methods

Reagents and Antibodies

BFA and nocodazole were purchased from Sigma-Aldrich (St Louis, MO), dissolved in dimethyl sulfoxide (DMSO), and stored at –20°C as stock solutions of 10 mg ml^{-1} and 5 mg ml^{-1}, respectively. Geneticin (G418 sulfate) and zeocyn were obtained from Invitrogen Life Technologies (Burlington, Ontario, Canada). Sera 9D2 and 9D5 were raised in rabbits against GBF1 using a hexa-histidine-tagged form of the N terminal domain of human GBF1 encoded by the 5′ *Ssp1-Nhe*1 fragment of the human GBF1 cDNA cloned at the *Nhe*1 site of pRSET A (Invitrogen). The recombinant protein (residues 5-621 of hGBF1) was expressed and purified as described (Mansour et al., 1999). 9D2 and 9D5 were affinity-purified using antigen conjugated onto an Affigel-10 column (Bio-Rad Laboratories, Mississauga, Ontario, Canada) as described (Harlow and Lane, 1988) and used at 1:50 dilution for immunofluorescence (IF). Anti-BIG1 serum 9D3 (1:500 dilution) was described previously (Claude et al., 1999). Alexa488-conjugated anti-GBF1 (H154) and anti-BIG1 (9D3) antibodies were prepared as before (Claude et al., 1999) using Alexa Fluor™ 488 Protein Labeling Kit (A-10235) (Molecular Probes, Eugene, OR) and used at 1:100 dilution for IF. For IF, the following additional polyclonal antibodies were used: anti-GFP (L. G. Berthiaume, University of Alberta, Edmonton, Canada) at 1:500; anti-p58 [Molly 6 (Saraste et al., 1987); J. Saraste, University of Bergen, Bergen, Norway] at 1:100; anti-sec31 [(Tang et al., 2000); B. L. Tang, University of Georgia, Athens, GA] at 1:500. The following monoclonal antibodies were used: anti-p115 [clone 3A10 (Waters et al., 1992); G. Waters (Princeton University, Princeton, NJ)] at 1:1000; anti-β-COP [clone M3A5 (Allan and Kreis, 1986); Sigma-Aldrich, St Louis, MO] at 1:300; anti-clathrin (clone X22; ABR-Affinity BioReagents, Golden, CO) at 1:200; anti-VSVG [clone P5D4 (Kreis and Lodish, 1986); T. Hobman, University of Alberta, Edmonton, Canada] at 1:100. Secondary antibodies were: Alexa594-conjugated goat anti-rabbit and Alexa488 conjugated goat anti-mouse antibodies (Molecular Probes, Eugene, OR) at 1:600.

Cell culture and isolation of NRK cell lines expressing GFP tagged GBF1

The following cell lines were used in this study: Hela (ATCC CCL-2); NRK-52E cells (ATCC CRL-1571); COS-1 cells (ATCC CRL-1650). Cells were maintained in DMEM supplemented with 10% fetal bovine serum (FBS) (Sigma), 100 μg ml^{-1} penicillin G, 100 μg ml^{-1} streptomycin and 2 mM glutamine at 37°C in a 5% CO_2 incubator.

To generate N-terminal GFP-tagged GBF1, the *Eco*RV and *Sac*II fragment from pCEP4-GBF1 (Claude et al., 1999) was inserted into pEGFP-C1 (enhanced green fluorescent protein; Clontech, Palo Alto, CA) digested with *Sma*I and *Sac*I. The EGFP-GBF1 chimera contained a linker of 111 nucleotides encoding 37 amino acids between EGFP and GBF1. The *Nhe*I and *Not*I GFP-GBF1 encoding fragment was subcloned into the corresponding sites of pIND (Invitrogen, Carlsbad, CA) to yield pIND-GFP-GBF1. To generate stable lines, pIND-GFP-GBF1 was co-electroporated into NRK cells with plasmid pVgRXR (Invitrogen). Transfectants harboring both plasmids were selected by growing cells in the presence of 400 μg ml^{-1} G418 and 200 μg ml^{-1} zeocyn. Expanded colonies were stored frozen until needed. Upon thawing, only a subset of colonies expressed GFP tagged GBF1, and in these only a fraction of the cells gave GFP signal. The clone with largest fraction of GFP-positive cells was chosen for further analysis. Two rounds of fluorescence activated cell sorting yielded a population with a greatly increased fraction (70%) of stably expressing cells. These cells, termed NRK-GFP-GBF1 remained heterogeneous: approximately 70% of cells express weak to moderate levels of GFP-GBF1 (1.0-1.5 times over endogenous level). For unknown reasons, ecdysone does not induce GFP-GBF1 expression.

Immunofluorescence microscopy

Cells grown on glass coverslips were washed in phosphate buffered saline (PBS) and fixed with 3% paraformaldehyde in PBS at room temperature for 20 minutes. Cells double labeled with mouse and rabbit antibodies or with two rabbit primary antibodies were processed as described before (Zhao et al., 2002). For double labeling with two rabbit primary antibodies cells were first decorated with unlabelled polyclonal antibody for 90 minutes, followed by Alexa594 labeled anti-rabbit IgG for 60 minutes. Cells were incubated a second time for 60 minutes with the same unlabelled polyclonal antibody, prior to final labeling for 60 minutes with Alexa488-labelled BIG1 antiserum (9D3) or Alexa488-labelled GBF1 antiserum (H154). Several control experiments confirmed lack of cross-reaction.

Most images were obtained by standard IF with an Axioskop II microscope (Carl Zeiss, Thornwood, NY) equipped with a 63× objective (NA=1.4). To avoid artifacts due to shifts in register between measurements, merged images in Figs 1, 6 and 8 were acquired using a dual-band filter set (51009; Chroma Technologies) that can capture signals from red and green fluorophores simultaneously.

For Fig. 1Aa,b, Fig. 2Ba-f, Fig. 4C and Fig. 9, single slice confocal images were obtained with a LSM 510 microscope (Carl Zeiss) equipped with a 63× objective (NA=1.4) using 488 nm laser excitation and a 500-550 nm bandpass filter for Alexa488 and GFP, 543 nm laser excitation and a >560 nm longpass filter for Alexa594. Images in Fig. 2Bg-i, were acquired with a Zeiss Axiovert 200M

microscope equipped with an UltraVIEW ERS 3E spinning disk (Perkin Elmer) and a Hamamatsu 9100-50 Electron multiplier CCD digital camera. When two markers were imaged in the same cells, each fluorophore was excited and detected sequentially (multitrack mode) to avoid channel bleed-through. Laser intensity and filters were adjusted to give maximum signal but avoid saturation.

Time-lapse imaging

NRK-GFP-GBF1 cells were grown in CO_2 independent DMEM (Gibco Laboratories, Grand Island, NY) plus 10% FBS in a Delta T open dish (Bioptechs, Butler, PA) and imaged on the temperature-controlled stage of a Zeiss LSM510 confocal laser scanning microscope at 37°C. Uniform and stable temperature was maintained with a Delta T system, supplemented with heated lid and objective heater (Bioptechs). LSM510 software was used to control image acquisition and manipulation. Unless otherwise indicated, fluorescent structures were viewed in a single image plane with the pinhole fully opened to maximize signal capture. For Fig. 7, NRK-GFP-GBF1 cells were grown on Plastek Cultureware glass bottom microwell dishes (MatTek Corp) and imaged on the temperature-controlled stage of a Zeiss Axiovert 200M microscope equipped with an UltraVIEW ERS 3E spinning disk (Perkin Elmer). Images were captured with an Orca-AG camera (Hamamatsu Photonics) and processed with Ultraview Image Suite.

FRAP and quantification

FRAP experiments were performed on the temperature-controlled stage of a Zeiss LSM510 confocal microscope as described above. An initial pre-bleach image was taken prior to bleaching a region of interest (ROI) (outlined in figures) 30 times at 100% laser power (488 nm line). Recovery of fluorescence into the ROI was monitored at 2 second (cytosolic FRAP; 3A) or 5 second (all others) intervals by scanning at 1% laser power. No significant focal level change or photo-bleaching was observed during recovery.

Quantitative analysis of recovery kinetics of GFP-GBF1 signal in the ROI (juxtanuclear Golgi region in Fig. 3B,D, Fig. 5A; cytoplasm in Fig. 3A, Fig. 5B) was performed on curves in which ROI intensity at each time point was expressed as a fraction of total cell fluorescence. Ratios at each time point were expressed as a fraction of the initial value before bleach (set as 1) and plotted against time, setting time zero as equal to the first time point after bleach. The data was then fit to the general equation $y=a\times(1-e^{-bx}) + c$ using KaleidaGraph (version 3.6.1, Synergy Software, Reading, PA). Note that the first two time points after bleach that correspond to fast diffusion of free cytosolic GFP-GBF1 were excluded from analysis to yield a single exponential. Recovery half times ($t_{1/2}$) were calculated as: $t_{1/2}=\ln 2/b$. The mobile fraction (R) can calculated from the relative ROI per total cell ratio after full recovery (a) and the relative ratio just after bleaching (Y_0) as: $R=(a-Y_0)/(1-Y_0)$.

Diffusion coefficient

Diffusion coefficients of GBF1 on the ER or in cytosol were determined by computer analysis of FRAP data as described in (Siggia et al., 2000) and (Sciaky et al., 1997). Briefly, ROI of 3 microns in diameter located within flat regions away from the nucleus were photobleached. Total fluorescence within ROI was measured as a function of time. Diffusion coefficients were determined by comparing recovery curve to a simulated recovery curve, and appropriately scaling the temporal axis for a least-squared best fit, with spatial units provided in microns/pixel. The procedure was completely automated using algorithms and software provided by E. Siggia et al. (Siggia et al., 2000).

BFA recruitment assays

BFA-mediated membrane recruitment of GBF1 was assayed using 3×150 mm plates of NRK cells. Following trypsinization, complete media was added and cells were pelleted by centrifugation at 1000 ***g*** for 1 minute (4°C). Cells were washed in buffer (10 mM Tris pH 8, 150 mM NaCl, protease inhibitor cocktail (Roche), pepstatin A and O-phenanthroline), containing either 0.5 μg ml^{-1} or 5 μg ml^{-1} BFA, or vehicle control (DMSO). Pelleted cells were resuspended in 5 volumes of wash buffer containing either 0.5 μg ml^{-1} or 5 μg ml^{-1} BFA, or DMSO. Following 5 minute incubation on ice, samples were homogenized by 15 passages through a 23 gauge needle. Low speed supernatants (1000 ***g*** for 1 minute, 4°C) were subsequently centrifuged at 115,000 ***g*** for 5 minutes (4°C). Resultant supernatants (cytosol) were retained and NP40 added to 1%. High-speed pellets (microsomes) were resuspended with equivalent volume of wash buffer containing 1% NP40. Equivalent amounts of cytosolic and microsomal fractions were separated by Tris-Glycine SDS-polyacrylamide electrophoresis, on 5% gels calibrated with prestained molecular weight standards (Bio-Rad). Following electrophoresis, proteins were transferred to nitrocellulose membranes, immunoblotted with primary antibodies, and detected using the ECL-plus system (Amersham Pharmacia Biosciences). Digital images were captured using a FluorChem 8000 imaging system (AlphaInnotech Corp, San Leandro, CA).

VSVtsO45 infection

COS-1 cells were grown to confluence on glass coverslips. Cells were infected with VSVts045 in CO_2-independent DMEM without FBS at 32°C for 1 hour. Infected cells were incubated at the restrictive temperature (40.5°C) for 3 hours post-infection in DMEM with 10% FCS to accumulate newly synthesized G-protein in the ER. VSVG protein was released by incubation at the permissive temperature (32°C) for the indicated time periods, prior to fixation and processing.

Microinjection

Before microinjection, affinity purified anti-GBF1 antibodies to be used were concentrated to ~20 mg ml^{-1} in PBS and cleared by passage through a 0.22 μm filter. Hela cells were grown to ~80% confluency on glass coverslips, and antibodies were injected into the cytoplasm with an Eppendorf semi automated microinjector and Femtotip needles (Brinkmann Instruments Inc., Westbury, NY). Injections were performed on a Nikon TE300 inverted microscope. After microinjection, cells were returned to the incubator for 2 hours prior to fixation and processing.

We thank B. P. Zhao for the construction, expression and preparation of recombinant proteins used for generation of GBF1-specific antisera; A. Gillchrist for preparation of recombinant proteins used for affinity purification of GBF1-specific antisera, as well as for maintenance of cultured cells; H. Chan for her insights and helpful advice in developing the procedures for live imaging experiments; X. Sun for antibody microinjection; F. Manolea for helpful comments on the manuscript. This study was supported by a grant (P.M.) from the Canadian Institutes of Health Research. X.Z. was supported by a studentship from the CIHR and from AHFMR. J.C. is a recipient of a General Award (University of Alberta). D.S. was supported by a grant from the Human Frontiers of Science Program (PM). A.C. was funded for the last part of the work by the Fondecyt project No. 1030346.

References

Allan, V. J. and Kreis, T. E. (1986). A microtubule-binding protein associated with membranes of the Golgi apparatus. *J. Cell Biol.* **103**, 2229-2239.

Altan-Bonnet, N., Sougrat, R. and Lippincott-Schwartz, J. (2004). Molecular basis for Golgi maintenance and biogenesis. *Curr. Opin. Cell Biol.* **16**, 364-372.

Aridor, M. and Balch, W. E. (1995). Principles of selective transport: coat complexes hold the key. *Trends Cell Biol.* **6**, 315-320.

Bannykh, S. I. and Balch, W. E. (1997). Membrane dynamics at the endoplasmic reticulum-Golgi interface. *J. Cell Biol.* **138**, 1-4.

Bednarek, S. Y., Ravazzola, M., Hosobuchi, M., Amherdt, M., Perrelet, A., Schekman, R. and Orci, L. (1995). COPI- and COPII-coated vesicles bud directly from the endoplasmic reticulum in yeast. *Cell* **83**, 1183-1196.

Beraud-Dufour, S., Paris, S., Chabre, M. and Antonny, B. (1999). Dual interaction of ADP ribosylation factor 1 with Sec7 domain and with lipid membranes during catalysis of guanine nucleotide exchange. *J. Biol. Chem.* **274**, 37629-37636.

Bergmann, J. E. (1989). Using temperature-sensitive mutants of VSV to study membrane protein biogenesis. *Methods Cell Biol.* **32**, 85-110.

Chardin, P., Paris, S., Antonny, B., Robineau, S., Beraud-Dufour, S., Jackson, C. L. and Chabre, M. (1996). A human exchange factor for ARF contains Sec7- and pleckstrin-homology domains. *Nature* **384**, 481-484.

Cherfils, J. and Melancon, P. (2005). On the action of Brefeldin A on Sec7-stimulated membrane-recruitment and GDP/GTP exchange of ARF proteins. *Biochem. Soc. Trans.* **33**, 635-638.

Claude, A., Zhao, B. P., Kuziemsky, C. E., Dahan, S., Berger, S. J., Yan, J. P., Armold, A. D., Sullivan, E. M. and Melancon, P. (1999). GBF1: A novel Golgi-associated BFA-resistant guanine nucleotide exchange factor that displays specificity for ADP-ribosylation factor 5. *J. Cell Biol.* **146**, 71-84.

Cole, N. B., Smith, C. L., Sciaky, N., Terasaki, M., Edidin, M. and Lippincott-Schwartz, J. (1996). Diffusional mobility of Golgi proteins in membranes of living cells. *Science* **273**, 797-801.

Cox, R., Mason-Gamer, R. J., Jackson, C. L. and Segev, N. (2004). Phylogenetic analysis of Sec7-domain-containing ARF nucleotide exchangers. *Mol. Biol. Cell* **15**, 1487-1505.

Donaldson, J. G., Lippincott-Schwartz, J., Bloom, G. S., Kreis, T. E. and Klausner, R. D. (1990). Dissociation of a 110-kD peripheral membrane protein from the Golgi apparatus is an early event in brefeldin A action. *J. Cell Biol.* **111**, 2295-2306.

Donaldson, J. G., Lippincott-Schwartz, J. and Klausner, R. D. (1991). Guanine nucleotides modulate the effects of brefeldin A in semipermeable cells: regulation of the association of a 110-kD peripheral membrane protein with the Golgi apparatus. *J. Cell Biol.* **112**, 579-588.

Garcia-Mata, R., Szul, T., Alvarez, C. and Sztul, E. (2003). ADP-ribosylation factor/COPI-dependent events at the endoplasmic reticulum-Golgi interface are regulated by the guanine nucleotide exchange factor GBF1. *Mol. Biol. Cell* **14**, 2250-2261.

Goldberg, J. (1998). Structural basis for activation of ARF GTPase: mechanisms of guanine nucleotide exchange and GTP-myristoyl switching. *Cell* **95**, 237-248.

Griffiths, G., Pepperkok, R., Locker, J. K. and Kreis, T. E. (1995). Immunocytochemical localization of beta-COP to the ER-Golgi boundary and the TGN. *J. Cell Sci.* **108**, 2839-2856.

Guo, Q., Vasile, E. and Krieger, M. (1994). Disruptions in Golgi structure and membrane traffic in a conditional lethal mammalian cell mutant are corrected by epsilon-COP. *J. Cell Biol.* **125**, 1213-1224.

Harlow, E. and Lane, D. (1988). *Antibodies, A Laboratory Manual*. Cold Spring Harbor: Cold Spring Harbor Laboratory Press.

Hauri, H. P., Kappeler, F., Andersson, H. and Appenzeller, C. (2000). ERGIC-53 and traffic in the secretory pathway. *J. Cell Sci.* **113**, 587-596.

Kawamoto, K., Yoshida, Y., Tamaki, H., Torii, S., Shinotsuka, C., Yamashina, S. and Nakayama, K. (2002). GBF1, a guanine nucleotide exchange factor for ADP-ribosylation factors, is localized to the cis-Golgi and involved in membrane association of the COPI coat. *Traffic* **3**, 483-495.

Klausner, R. D., Donaldson, J. G. and Lippincott-Schwartz, J. (1992). Brefeldin A: insights into the control of membrane traffic and organelle structure. *J. Cell Biol.* **116**, 1071-1080.

Klumperman, J., Schweizer, A., Clausen, H., Tang, B. L., Hong, W., Oorschot, V. and Hauri, H. P. (1998). The recycling pathway of protein ERGIC-53 and dynamics of the ER-Golgi intermediate compartment. *J. Cell Sci.* **111**, 3411-3425.

Kreis, T. E. and Lodish, H. F. (1986). Oligomerization is essential for transport of vesicular stomatitis viral glycoprotein to the cell surface. *Cell* **46**, 929-937.

Lee, M. C., Miller, E. A., Goldberg, J., Orci, L. and Schekman, R. (2004). Bi-directional protein transport between the ER and Golgi. *Annu. Rev. Cell Dev. Biol.* **20**, 87-123.

Letourneur, F., Gaynor, E. C., Hennecke, S., Demolliere, C., Duden, R., Emr, S. D., Riezman, H. and Cosson, P. (1994). Coatomer is essential for retrival of dilysine-tagged proteins to the endoplasmic reticulum. *Cell* **79**, 1199-1207.

Lippincott-Schwartz, J., Yuan, L. C., Bonifacino, J. S. and Klausner, R. D. (1989). Rapid redistribution of Golgi proteins into the ER in cells treated with brefeldin A: evidence for membrane cycling from Golgi to ER. *Cell* **56**, 801-813.

Majoul, I., Sohn, K., Wieland, F. T., Pepperkok, R., Pizza, M., Hillemann, J. and Soling, H. D. (1998). KDEL receptor (Erd2p)-mediated retrograde transport of the cholera toxin A subunit from the Golgi involves COPI, p23, and the COOH terminus of Erd2p. *J. Cell Biol.* **143**, 601-612.

Mansour, S. J., Skaug, J., Zhao, X. H., Giordano, J., Scherer, S. W. and Melancon, P. (1999). p200 ARF-GEP1: a Golgi-localized guanine nucleotide exchange protein whose Sec7 domain is targeted by the drug brefeldin A. *Proc. Natl. Acad. Sci. USA* **96**, 7968-7973.

Martinez-Menarguez, J. A., Geuze, H. J., Slot, J. W. and Klumperman, J. (1999). Vesicular tubular clusters between the ER and Golgi mediate concentration of soluble secretory proteins by exclusion from COPI-coated vesicles. *Cell* **98**, 81-90.

Melancon, P., Zhao, X. and Lasell, T. K. (2004). Large ARF-GEFs of the Golgi complex: in search of mechanisms for the cellular effects of BFA. In *ARF Family GTPases*. Vol. 1 (ed. R. A. Kahn), pp. 101-119. Dordrecht: Kluwer Academic Publishers.

Mogelsvang, S., Marsh, B. J., Ladinsky, M. S. and Howell, K. E. (2004). Predicting function from structure: 3D structure studies of the mammalian Golgi complex. *Traffic* **5**, 338-345.

Mossessova, E., Corpina, R. A. and Goldberg, J. (2003). Crystal structure of ARF1*Sec7 complexed with Brefeldin A and its implications for the guanine nucleotide exchange mechanism. *Mol. Cell* **12**, 1403-1411.

Mouratou, B., Biou, V., Joubert, A., Cohen, J., Shields, D. J., Geldner, N., Jurgens, G., Melancon, P. and Cherfils, J. (2005). The domain architecture of large guanine nucleotide exchange factors for the small GTP-binding protein ARF. *BMC Genomics* **6**, 20.

Niu, T. K., Pfeifer, A. C., Lippincott-Schwartz, J. and Jackson, C. L. (2005). Dynamics of GBF1, a brefeldin A-sensitive ARF1 exchange factor at the Golgi. *Mol. Biol. Cell* **16**, 1213-1222.

Oprins, A., Duden, R., Kreis, T. E., Geuze, H. J. and Slot, J. W. (1993). Beta-COP localizes mainly to the cis-Golgi side in exocrine pancreas. *J. Cell Biol.* **121**, 49-59.

Orci, L., Glick, B. S. and Rothman, J. E. (1986). A new type of coated vesicular carrier that appears not to contain clathrin: its possible role in protein transport within the Golgi stack. *Cell* **46**, 171-184.

Orci, L., Stamnes, M., Ravazzola, M., Amherdt, M., Perrelet, A., Sollner, T. H. and Rothman, J. E. (1997). Bidirectional transport by distinct populations of COPI-coated vesicles. *Cell* **90**, 335-349.

Orci, L., Perrelet, A. and Rothman, J. E. (1998). Vesicles on strings: morphological evidence for processive transport within the Golgi stack. *Proc. Natl. Acad. Sci. USA* **95**, 2279-2283.

Ostermann, J., Orci, L., Tani, K., Amherdt, M., Ravazzola, M., Elazar, Z. and Rothman, J. E. (1993). Stepwise assembly of functionally active transport vesicles. *Cell* **75**, 1015-1025.

Pepperkok, R., Scheel, J., Horstmann, H., Hauri, H. P., Griffiths, G. and Kreis, T. E. (1993). Beta-COP is essential for biosynthetic membrane transport from the endoplasmic reticulum to the Golgi complex in vivo. *Cell* **74**, 71-82.

Peter, F., Plutner, H., Zhu, H., Kreis, T. E. and Balch, W. E. (1993). Beta-COP is essential for transport of protein from the endoplasmic reticulum to the Golgi in vitro. *J. Cell Biol.* **122**, 1155-1167.

Peyroche, A., Antonny, B., Robineau, S., Acker, J., Cherfils, J. and Jackson, C. L. (1999). Brefeldin A acts to stabilize an abortive ARF-GDP-Sec7 domain protein complex: involvement of specific residues of the Sec7 domain. *Mol. Cell* **3**, 275-285.

Presley, J. F., Cole, N. B., Schroer, T. A., Hirschberg, K., Zaal, K. J. and Lippincott-Schwartz, J. (1997). ER-to-Golgi transport visualized in living cells. *Nature* **389**, 81-85.

Presley, J. F., Ward, T. H., Pfeifer, A. C., Siggia, E. D., Phair, R. D. and Lippincott-Schwartz, J. (2002). Dissection of COPI and ARF1 dynamics in vivo and role in Golgi membrane transport. *Nature* **417**, 187-193.

Rabouille, C. and Klumperman, J. (2005). Opinion: the maturing role of COPI vesicles in intra-Golgi transport. *Nat. Rev. Mol. Cell Biol.* **6**, 812-817.

Renault, L., Guibert, B. and Cherfils, J. (2003). Structural snapshots of the mechanism and inhibition of a guanine nucleotide exchange factor. *Nature* **426**, 525-530.

Saraste, J., Palade, G. E. and Farquhar, M. G. (1987). Antibodies to rat pancreas Golgi subfractions: identification of a 58-kD cis-Golgi protein. *J. Cell Biol.* **105**, 2021-2029.

Scales, S. J., Pepperkok, R. and Kreis, T. E. (1997). Visualization of ER-to-Golgi transport in living cells reveals a sequential mode of action for COPII and COPI. *Cell* **90**, 1137-1148.

Scheel, J., Pepperkok, R., Lowe, M., Griffiths, G. and Kreis, T. E. (1997). Dissociation of coatomer from membranes is required for brefeldin A-induced transfer of Golgi enzymes to the endoplasmic reticulum. *J. Cell Biol.* **137**, 319-333.

Sciaky, N., Presley, J., Smith, C., Zaal, K. J., Cole, N., Moreira, J. E., Terasaki, M., Siggia, E. and Lippincott-Schwartz, J. (1997). Golgi tubule traffic and the effects of brefeldin A visualized in living cells. *J. Cell Biol.* **139**, 1137-1155.

Shima, D. T., Scales, S. J., Kreis, T. E. and Pepperkok, R. (1999). Segregation of COPI-rich and anterograde-cargo-rich domains in endoplasmic-reticulum-to-Golgi transport complexes. *Curr. Biol.* **9**, 821-824.

Shinotsuka, C., Waguri, S., Wakasugi, M., Uchiyama, Y. and Nakayama, K. (2002). Dominant-negative mutant of BIG2, an ARF-guanine nucleotide exchange factor, specifically affects membrane trafficking from the trans-Golgi network through inhibiting membrane association of AP-1 and GGA coat proteins. *Biochem. Biophys. Res. Commun.* **294**, 254-260.

Siggia, E. D., Lippincott-Schwartz, J. and Bekiranov, S. (2000). Diffusion in inhomogeneous media: theory and simulations applied to whole cell photobleach recovery. *Biophys. J.* **79**, 1761-1770.

Spang, A., Herrmann, J. M., Hamamoto, S. and Schekman, R. (2001). The ADP ribosylation factor-nucleotide exchange factors Gea1p and Gea2p have overlapping, but not redundant functions in retrograde transport from the Golgi to the endoplasmic reticulum. *Mol. Biol. Cell* **12**, 1035-1045.

Stephens, D. J. and Pepperkok, R. (2002). Imaging of procollagen transport reveals COPI-dependent cargo sorting during ER-to-Golgi transport in mammalian cells. *J. Cell Sci.* **115**, 1149-1160.

Stephens, D. J., Lin-Marq, N., Pagano, A., Pepperkok, R. and Paccaud, J. P. (2000). COPI-coated ER-to-Golgi transport complexes segregate from COPII in close proximity to ER exit sites. *J. Cell Sci.* **113**, 2177-2185.

Szul, T., Garcia-Mata, R., Brandon, E., Shestopal, S., Alvarez, C. and Sztul, E. (2005). Dissection of membrane dynamics of the ARF-guanine nucleotide exchange factor GBF1. *Traffic* **6**, 374-385.

Tang, B. L., Zhang, T., Low, D. Y., Wong, E. T., Horstmann, H. and Hong, W. (2000). Mammalian homologues of yeast sec31p. An ubiquitously expressed form is localized to endoplasmic reticulum (ER) exit sites and is essential for ER-Golgi transport. *J. Biol. Chem.* **275**, 13597-13604.

Tang, B. L., Wang, Y., Ong, Y. S. and Hong, W. (2005). COPII and exit from the endoplasmic reticulum. *Biochim. Biophys. Acta* **1744**, 293-303.

Torii, S., Banno, T., Watanabe, T., Ikehara, Y., Murakami, K. and Nakayama, K. (1995). Cytotoxicity of brefeldin A correlates with its inhibitory effect on membrane binding of COP coat proteins. *J. Biol. Chem.* **270**, 11574-11580.

Ward, T. H., Polishchuk, R. S., Caplan, S., Hirschberg, K. and Lippincott-Schwartz, J. (2001). Maintenance of Golgi structure and function depends on the integrity of ER export. *J. Cell Biol.* **155**, 557-570.

Waters, M. G., Serafini, T. and Rothman, J. E. (1991). 'Coatomer': a cytosolic protein complex containing subunits of non- clathrin-coated Golgi transport vesicles. *Nature* **349**, 248-251.

Waters, M. G., Clary, D. O. and Rothman, J. E. (1992). A novel 115-kD peripheral membrane protein is required for intercisternal transport in the Golgi stack. *J. Cell Biol.* **118**, 1015-1026.

Wey, C. L., Cone, R. A. and Edidin, M. A. (1981). Lateral diffusion of rhodopsin in photoreceptor cells measured by fluorescence photobleaching and recovery. *Biophys. J.* **33**, 225-232.

Xu, D. and Hay, J. C. (2004). Reconstitution of COPII vesicle fusion to generate a pre-Golgi intermediate compartment. *J. Cell Biol.* **167**, 997-1003.

Yan, J. P., Colon, M. E., Beebe, L. A. and Melancon, P. (1994). Isolation and characterization of mutant CHO cell lines with compartment-specific resistance to brefeldin A. *J. Cell Biol.* **126**, 65-75.

Zeuschner, D., Geerts, W. J., van Donselaar, E., Humbel, B. M., Slot, J. W., Koster, A. J. and Klumperman, J. (2006). Immuno-electron tomography of ER exit sites reveals the existence of free COPII-coated transport carriers. *Nat. Cell Biol.* **8**, 377-383.

Zhao, X., Lasell, T. K. and Melancon, P. (2002). Localization of large ADP-ribosylation factor-guanine nucleotide exchange factors to different Golgi compartments: evidence for distinct functions in protein traffic. *Mol. Biol. Cell* **13**, 119-133.